The paper was published in the proceedings of the 11th Australia New Zealand Conference on Geomechanics and was edited by Prof. Guillermo Narsilio, Prof. Arul Arulrajah and Prof. Jayantha Kodikara. The conference was held in Melbourne, Australia, 15-18 July 2012.

Geotechnical Characterisation of Compacted Ground: Forward Modelling of the HVSR Curve

P. Harutoonian[1], C. J. Leo[1], S. Liyanapathirana[1], R. Golaszewski[2] and R. Moyle[3]

[1]School of Engineering, University of Western Sydney, Locked Bag 1797, Penrith, NSW 2751; PH (02) 4736 0979; FAX (02) 4736 0833; email: p.harutoonian@uws.edu.au, c.leo@uws.edu.au, s.liyanapathirana@uws.edu.au
[2]Penrith Lakes Development Corporation, PO Box 457, Cranebrook NSW 2749; PH (02) 4734 8106; FAX (02) 4730 1462; email: robert.golaszewski@pldc.com.au
[3]Coffey Geotechnics Pty Ltd, PO Box 125 North Ryde NSW 1670; PH (02) 9911 1000; FAX (02) 9911 1001; email: richard_moyle@coffey.com

ABSTRACT

The passive Horizontal-to-Vertical Spectral Ratio (HVSR) technique has been investigated as a means to assess and monitor compaction at a large quarry site in Western Sydney. The quarry has undergone extensive rehabilitation in the form of filling and compaction works to return the site to parkland status with the possibility of new housing development in some areas. Density (proctor, nuclear density gauge) and invasive penetration tests (SPT, CPT, DMT) have been performed to assess the quality of the compacted ground. However, the range of the density test is limited to a depth of one metre at most, and the unit cost of the invasive mechanical test is high, particularly when dealing with a large quarry site with deep layers of compaction. Consequently, the fast and low cost passive ambient noise HVSR technique has been proposed using two approaches to characterise the ground compaction. The first approach, by directly interpreting the measured HVSR data has been described in a companion paper, whereas the second approach, by forward modelling of measured HVSR data will be discussed in the current paper. The second approach is applied to estimate both the shear wave velocity (V_s) and the soil layering thickness (h) indicating the structure of the compacted ground.

Keywords: Compaction, HVSR, Forward Modelling, Microtremors, Shear Wave Velocity (V_s)

1 INTRODUCTION

A study has been initiated to investigate the use of the passive ambient noise Horizontal-to-Vertical Spectral Ratio (HVSR) technique to characterise compacted ground. Measurements of the ambient vibrations in 3 orthogonal directions (2 horizontal and 1 vertical components) were made by using a compact, standalone battery operated, lightweight (about 1kg) and high-resolution electro-dynamic sensor. The main attributes of this technique are speed and portability, in comparison to mechanical and other surface wave methods. Moreover, the theoretical basis of the HVSR technique is uniquely different to the other surface wave methods, such as the SASW, MASW and ReMi techniques proposed in recent years. The former, as the name implies, relies on the measurement of the HVSR curve, and the latter on the phase velocity dispersion curve.

The passive ambient noise HVSR technique has been applied to a very large quarry site in Western Sydney that has been compacted by different methods up to depths of 14 m. At each station over dynamically- or roller-compacted areas of the site, 16 minutes of ambient noise measurements were taken. Techniques have been developed to infer the compaction quality of these areas by (1) directly interpreting the measured HVSR curves as well as by (2) forward modelling of the HVSR curves to derive the shear wave velocity (V_s) profile. The work in (1) has been discussed in a companion paper, whereas the current paper concentrates on the work in (2).

Forward modelling of the measured HVSR curve was applied to infer the layering V_s and thicknesses (y) of the ground. However, initial calibration with mechanical methods (e.g. boreholes, SPT, CPT, etc) is essential to ensure correct interpretation of measured data. Once calibrated, the HVSR technique can be utilised to 'fill the gaps' left out by the mechanical testing. The V_s profile reflects the stiffness of the ground and can be correlated to other useful geotechnical properties (e.g. SPT (N) (e.g. Hasancebi & Ulusay 2007), *CPT* (q_c) (e.g. Karray et al. 2011), density (ρ_d) (e.g. Kim et al. 2001), bearing capacity (q_a) (e.g. Tezcan et al. 2006), etc).

2 METHODOLOGY

The test site and the method used to measure the microtremors in the ground (to produce the measured HVSR curve) have been discussed in the companion paper (Harutoonian et al. 2012).

2.1 Theoretical Model of the HVSR Curve

The theoretical model applied in the present paper is based on the work of Lunedei and Albarello (2009) and Arai and Tokimatsu (2004). The model is used to compute the Rayleigh- and Love- surface wave propagation in multi-layered viscoelastic media resulting from randomly distributed independent ambient noise sources which comprise vertical and horizontal harmonic point forces on the ground surface. Due to the stochastic random nature of the noise sources, the theoretical HVSR at angular frequency, ω, is defined as the ratio of average power components in the horizontal and vertical directions. This is expressed in terms of variances of the horizontal and vertical vibrations: V_H and V_v so that:

$$HVSR(\omega)_S = \sqrt{\frac{v_H(\omega)}{v_V(\omega)}} \tag{1}$$

2.2 Forward Modelling to Infer the Shear Wave Velocity (V_s) Profile

In his seminal paper, Nakamura (1989) suggested that the horizontal to vertical spectral ratio (HVSR) of the surface microtremors reflect the transfer function of the surface layers. The peaks observed in the measured HVSR curve could be generally explained by the presence of impedance contrasts of soil layers. Thus, typically, an observed peak on a HVSR curve would suggest that there is a change in the impedance (ρV_s) of the material, such that the higher the peak, the greater will be the corresponding change in the impedance. Hence, the measured HVSR curves reflect the soil layering (profile) of the site. The soil layering data, however, must be extracted from the measured HVSR curves in a process known as the “forward modelling of the HVSR curves”. This proceeds as follows: the theoretical model of the soil layering (using 6 soil parameters) is used to compute a theoretical HVSR curve which is then adjusted to fit the measured HVSR curve of the site by making appropriate changes in the values of the soil parameters in the model. This process may continue over several iterations until sufficient convergence or fit is achieved. Although a total of 6 soil parameters are required for each soil layer in the model, the soil parameters that will most significantly influence the patterns of the HVSR curve are the V_s and layer thickness (y).

A theoretical simulation below illustrates how impedance contrasts in the ground can be related to peaks observed on the HVSR curve.

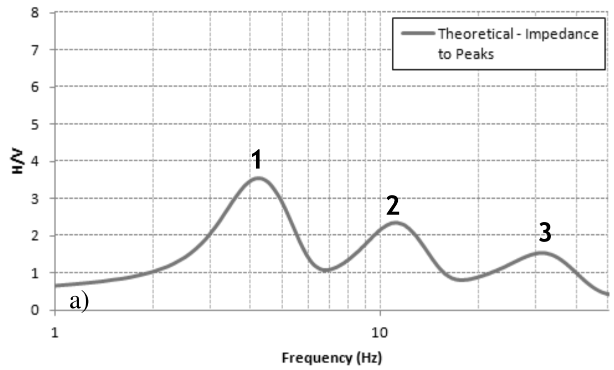

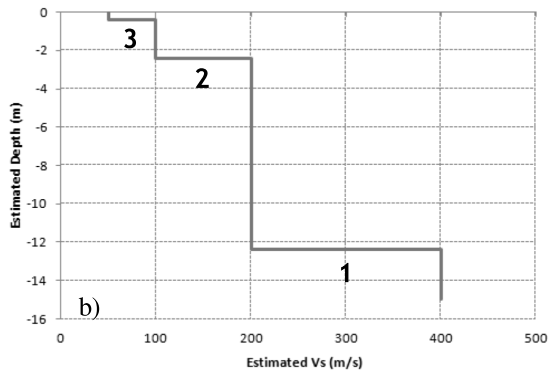

Figure 1. Theoretical HVSR curve – (a) peaks to (b) impedance contrasts

Here a simple soil profile shown in Figure 1(b) is used to generate the theoretical HVSR curve shown in Figure 1a. The soil profile shows a four-layer system, where the V_s values are increasing (factor of 2) with depth and the layer thicknesses are also increasing (factor of 5) with depth. The bulk densities of the soil layers generally do not vary much and are assumed to remain at a constant. The generated theoretical HVSR curve (Figure 1a) shows 3 obvious peaks (labelled as “1”, “2” and “3”) which can be linked to the 3 impedance contrasts at the interfaces “1”, “2” and “3” shown in the soil profile in Figure

1b. This simple simulation identifies not only a link between the predominant peak "1" on the HVSR curve with the impedance contrast between the bedrock and overlying fill layers (i.e. between soil below and above the interface "1" in the soil profile) but also the links for the secondary peaks observed at higher frequencies. The secondary peaks identifying the impedance contrasts at the more shallow layers, in particular, have been investigated in this study as a means to assess ground compaction at the quarry site.

3 EXPERIMENTAL RESULTS

3.1 Normalisation of V_s and q_c for Overburden Stress

Good correlations have been established between normalised V_s and dry density (ρ_d) of compacted ground in earlier studies (e.g. Kim et al. 2001; Karray et al. 2011). These results suggest that the normalised V_s could be applied in lieu of the dry density to assess compaction quality. Thus in this study, the inferred V_s have been normalised using the equation below proposed by Robertson et al. (1992):

$$V_{sn} = V_{sm}\left(\frac{P_a}{\sigma'_v}\right)^{0.25} \quad (2)$$

where, V_{sn} is the resulting normalised shear wave velocity, V_{sm} is the derived/measured shear wave velocity, P_a is the reference/atmospheric pressure (assumed as 100 kPa) and $\sigma'_v = \gamma' z$ is the vertical effective stress (in kPa), γ' is the effective unit weight of the surface layer and z is the depth. Bore log data was used to estimate the unit weights of the compacted material. Furthermore, equation (3) from Robertson et al. (1992) was used to normalise the CPT 'q_c' values against overburden stress:

$$q_{cn} = q_{cm}\left(\frac{P_a}{\sigma'_v}\right)^{0.5} \quad (3)$$

where, q_{cn} is the normalised cone end resistance and q_{cm} is the measured cone end resistance.

3.2 Dynamic Compaction

The measured and theoretical HVSR curves at two stations (C3 and E1) in the dynamic compaction (DC) area are shown in Figures 2a and b to illustrate the goodness-of-fit between theory and measurements by a trial-and-error approach. The theoretical HVSR curves were computed by the theoretical model with a soil model where the layer thicknesses were constrained to a narrow range based on the data available from the bore logs. This approach has been found to work quite well in this study. Similar results regarding the goodness-of-fit were achieved for the remaining locations in the DC area. However, not all results could be presented here due to a limitation of space.

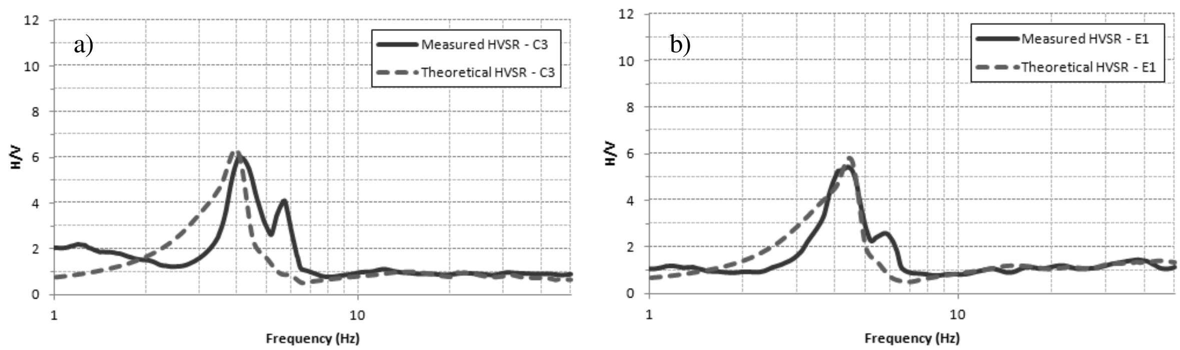

Figure 2. DC forward modelling of HVSR curves at – (a) station C3 and (b) station E1

The fitting of the theoretical HVSR curve to the measured HVSR curve allowed the V_s profile of the compaction to be inferred. To further verify the accuracy of the fitting, the normalised V_s profiles have been benchmarked against the closest available mechanical CPT (after normalisation using equation

3) and DMT results which are interspersed in the DC area. Figures 3a and b show the superposed normalised V_S profiles (at C3 and E1) on both the CPT and DMT data from the locations, BH 9.2 and BH 9.4 respectively. The results in Figures 3a and b exemplify the consistent relative stratigraphy between the normalised V_s profiles and the invasive cone resistance 'q_c' from the CPT. Moreover, the V_s and CPT results are also consistent with the constrained modulus '*M*' from the DMT.

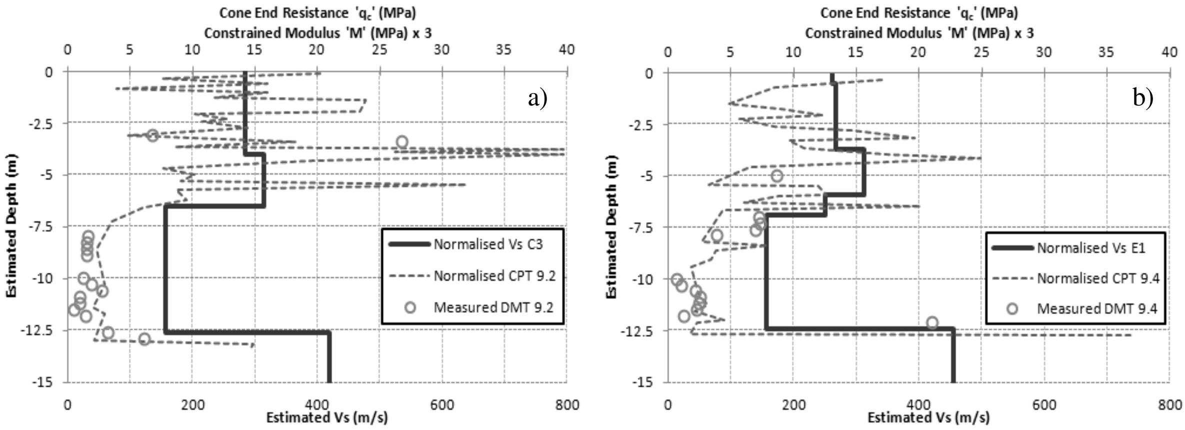

Figure 3. DC V_s profile and verification with CPT and DMT at – (a) station C3 and (b) station E1

The companion paper (Harutoonian et al. 2012) established three main salient features in the raw measured HVSR curves. These could be corroborated by the V_s profiles shown in Figures 3a and b as follows:

1. Predominant resonance frequency f_0 peak at approximately 4.5 Hz is associated with the increase in V_s at a depth of approximately 12 – 13 m.
2. Trough between 6.5 and 10 Hz where the H/V ratio dips below one in the HVSR curves is verified as truly bearing the hallmarks of an embedded softer soil layer and not due to the Rayleigh wave ellipticity feature at $2f_0$ (at approximately 8 – 9 Hz). This is shown by the V_s drop at a depth of 7 m to approximately 12.5 m in the surface layers.
3. Smaller secondary peaks located at frequencies above 12 Hz, indicating smaller impedance contrasts between the near surface layers. This could be linked to the sizeable jumps in V_s at depths of roughly 0.5 m and 4 m.

The inferred V_s profiles at the stations not in the proximity of any mechanical CPT or DMT were used to establish the quality of the dynamic compaction in the gaps not covered by the mechanical tests. The profiles reveal uniformly consistent compaction throughout the compacted area, except at one station where the compaction was deemed marginally below the compaction measured at the borehole locations.

3.3 Roller Compaction

The measured and theoretical HVSR curves at stations X2 and Z1 in the roller compaction (RC) area are shown in Figures 4a and b. These illustrate the goodness-of-fit between theory and measurements for the RC area. The normalised V_s profiles for these stations are shown in Figure 5. After normalisation of the derived V_s values using equation (2), the profiles show a good level of uniformity in the compacted layers consistent with an area where the roller compaction has been rigorously controlled. The general uniformity in the normalised V_s profile in the compacted surface layers corroborate with the interpretation of the salient characteristics (highlighted in Harutoonian et al. 2012) of the RC area:

1. Predominant resonance frequency f_0 peak at approximately 5.1 Hz is associated with the increase in V_s at a depth of 14 m.
2. Presence of a trough at $2f_0$ in the HVSR curves is confirmed as due to Rayleigh wave ellipticity and not because of an embedded softer/looser layer in the surface layers.
3. Uniformity of the profiles is consistent with the interpretation that the relatively smooth and flat HVSR curves observed at higher frequencies (near surface) indicate a more uniform compaction.

The profiles of the HVSR stations in this area confirm the general uniformity and consistency of ground compaction achieved.

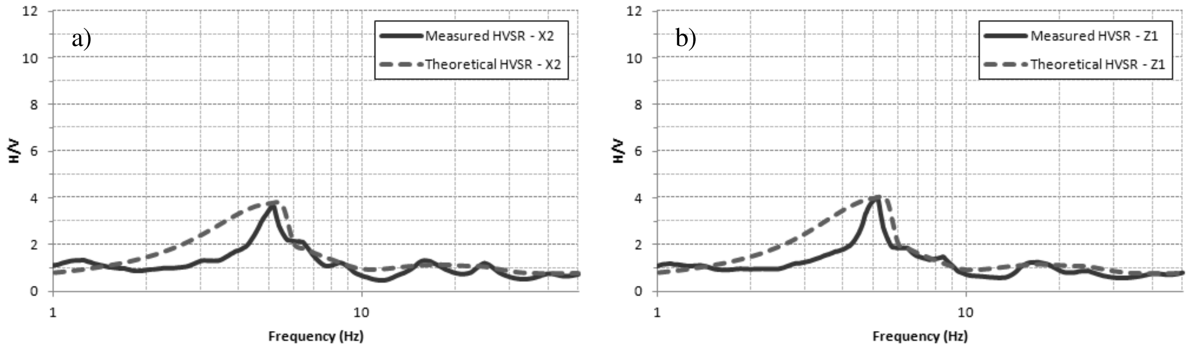

Figure 4. RC forward modelling of HVSR curves at – (a) station X2 and (b) station Z1

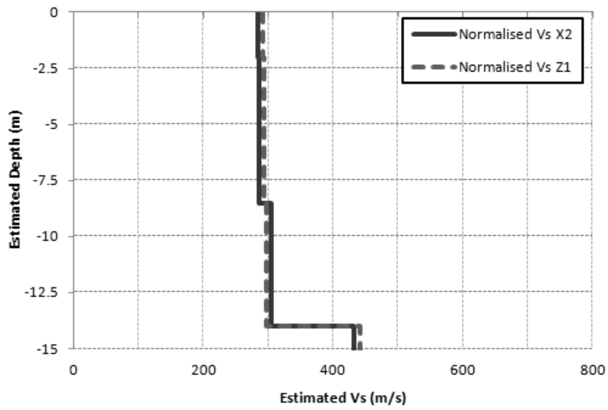

Figure 5. RC V_s profile – stations X2 and Z1

3.4 Comparison of Roller- and Dynamic- Compaction

The inferred V_s profiles provide a consistent basis to compare the quality of the roller- and dynamic-compacted areas. Table 1 shows the mean and standard deviation (σ) of the V_s data for every metre thick of compacted soil averaged over all stations for the respective DC and the RC areas. For the DC area, the compacted soil is taken to be from the ground surface to the depth of influence of the dynamic compaction (approximately 7 – 8 m). The compacted material for the RC area is taken to be from the ground surface to the bedrock (approximately 13 – 14m).

Table 1: Comparison of mean and variance of V_s of compacted material at the DC and RC areas

	DC Area		RC Area	
	Mean	**σ**	**Mean**	**σ**
Minimum	236	24.4	294	1.7
Maximum	288	70.6	306	19.4
Average	262	42.0	298	12.2

The outcome of the two compaction areas has been summarised in three ways:

1. Overall Compaction Quality – The overall mean of the RC area is higher than the DC area.
2. Lateral Variability – The RC area shows a lower level of lateral variability in the V_s profiles, relative to the DC area, as shown by the significantly lower variance (σ) in the V_s throughout the entire RC area.
3. Depth Wise Variability – The RC area shows better consistency depth wise than DC area. This can be seen in Figures (3a and b, and 5). As mentioned above, these figures represent typical V_s profiles from their respective areas. The V_s profiles not shown in this paper produce very similar outcomes.

4 CONCLUSION

The study has shown that the fast and operationally simple HVSR technique could be used to characterise compacted grounds, and especially to cover the gaps left by the localised invasive mechanical tests. In this way, soft/loose layers of compaction that may have been missed by the traditional quality control tests could be avoided. The approach of combining precise and expensive localised invasive mechanical techniques with a cost-effective but less precise HVSR technique would maximise the strengths and minimise the limitations of field testing needed to cover an extensive and deep site.

5 ACKNOWLEDGEMENTS

Pavlick Harutoonian is supported by a higher degree research PhD scholarship from the University of Western Sydney. This study is partially funded by the Australian Research Council (ARC), Penrith Lakes Development Corporation (PLDC) and Coffey Geotechnics Pty Ltd (Coffey). The authors gratefully acknowledge the kind assistance of Drew Bilbe (PLDC) and Michael Hughes (Coffey) throughout this study.

REFERENCES

Arai, H. & Tokimatsu, K. 2004, 'S-Wave velocity profiling by inversion of microtremor H/V spectrum', *Bulletin of the Seismological Society of America*, vol. 94, no. 1, pp. 53-63.

Harutoonian, P., Leo, C.J., Liyanapathirana, S., Golaszewski, R. & Moyle, R. 2012, 'Geotechnical Characterisation of Compacted Ground: Interpretation of the HVSR Curve', *ANZ2012*.

Hasancebi, N. & Ulusay, R. 2007, 'Empirical correlations between shear wave velocity and penetration resistance for ground shaking assessments', *Bulletin of Engineering Geology and the Environment* vol. 66, pp. 203-213.

Karray, M., Lefebvre, G., Ethier, Y. & Bigras, A. 2011, 'Influence of particle size on the correlation between shear wave velocity and cone tip resistance', *Canadian Geotechnical Journal*, vol. 48, pp. 599 - 615.

Kim, D.S., Shin, M.K. & Park, H.C. 2001, 'Evaluation of density in layer compaction using SASW method', *Soil Dynamics and Earthquake Engineering*, vol. 21, pp. 39 - 46.

Lunedei, E. & Albarello, D. 2009, 'On the seismic noise wavefield in a weakly dissipative layered earth', *Geophysical Journal International*, vol. 177, pp. 1001 - 1014.

Nakamura, Y. 1989, 'A method for dynamic characteristics estimation of subsurface using microtremor on the ground surface', *Quarterly Report of Railway Technical Research Institute (RTRI)*, vol. 30, no. 1, pp. 25 - 33.

Robertson, P.K., Woeller, D.J. & Finn, W.D.L. 1992, 'Seismic cone penetration test for evaluating liquefaction potential under cyclic loading', *Canadian Geotechnical Journal*, vol. 29, no. 4, pp. 686-695.

Tezcan, S.S., Keceli, A. & Ozdemir, Z. 2006, 'Allowable bearing capacity of shallow foundations based on shear wave velocity', *Geotechnical and Geological Engineering*, vol. 24, pp. 203 - 218.